Nuclear Instruments and Methods in Physics Research B 288 (2012) 10–17

Contents lists available at SciVerse ScienceDirect

Nuclear Instruments and Methods in Physics Research B

journal homepage: www.elsevier.com/locate/nimb

Elemental analysis of aerosols collected at the Pierre Auger Cosmic Ray Observatory with PIXE technique complemented with SEM/EDX

M.I. Micheletti [a,b,c,*], L.G. Murruni [d], M.E. Debray [e,f], M. Rosenbusch [c], M. Graf [a], G. Ávila Cadena [g,h], P. Vitale [g,h], J. Davidson [c,e], H. Somacal [e,f]

[a] Instituto de Física Rosario (IFIR) – CONICET/UNR, Bv. 27 de Febrero 210 bis (2000), Rosario, Argentina
[b] Facultad de Ciencias Bioquímicas y Farmacéuticas, Universidad Nacional de Rosario, UNR, Suipacha 531 (2000), Rosario, Argentina
[c] CONICET (Consejo Nacional de Investigaciones Científicas y Técnicas), Avda. Rivadavia 1917 (C1033AAJ), Ciudad Autónoma de Buenos Aires, Argentina
[d] Servicio Geológico Minero Argentino (SEGEMAR), Buenos Aires, Argentina
[e] Gerencia de Investigación y Aplicaciones, Comisión Nacional de Energía Atómica, Av. Gral. Paz 1499 (1650), San Martín, Buenos Aires, Argentina
[f] Universidad Nacional de Gral. San Martín, M. de Irigoyen 3100 (1650), San Martín, Buenos Aires, Argentina
[g] Comisión Nacional de Energía Atómica, Av. del Libertador 8250, Ciudad Autónoma de Buenos Aires, Argentina
[h] Pierre Auger Observatory, Av. San Martín Norte 304 (5613), Malargüe, Argentina

ARTICLE INFO

Article history:
Received 15 July 2011
Received in revised form 24 June 2012
Available online 25 July 2012

Keywords:
Elemental analysis
Aerosols
Auger Observatory
PIXE
SEM/EDX

ABSTRACT

The aim of this work is to characterize surface aerosols at the Pierre Auger Cosmic Ray Observatory located at Pampa Amarilla, near Malargüe city, in the Andes region of Argentina, with experimental sampling techniques used for the first time in a cosmic ray observatory, adding to information provided by the existing Auger aerosol monitors. A good knowledge of the optical attenuation due to aerosols is crucial for a good reconstruction of the signals from cosmic ray showers detected by the fluorescence detectors of the Observatory. Aerosols were collected in filters, during the Southern Hemisphere winter and spring in 2008. Concentrations in PM2.5 and PM2.5–10 filters were determined by gravimetric analysis and their elemental composition by the PIXE technique, complemented with SEM/EDX. Low aerosol concentrations were measured during the sampling period. The mean total mass PM10 (=PM2.5 + PM2.5–10 fractions) value was [mean(se)] 9.8(1.0) $\mu g/m^3$ [sd = 5.9 $\mu g/m^3$]. The mean PM10 value during winter was 7(1.1) $\mu g/m^3$ [sd = 4.5 $\mu g/m^3$], about half of the 13.1(1.5) [sd = 5.7 $\mu g/m^3$] measured during springtime. The PM2.5 fraction was approximately 30% of the PM10 fraction. PIXE results gave levels of S, Cl, K, Ca, Ti, Mn, Fe in the analyzed aerosol samples, showing that these elements correspond to 25% and 13% of the PM2.5 and PM2.5–10 total mass respectively. The rest of the mass was due to the elements with low Z (below 16) which cannot be detected by our X-ray setup. Comparison with SEM/EDX analysis showed that most of them were Si and Al (aluminosilicates). Our results indicate that most of the aerosols at the Auger Observatory would most likely come from the soil of the region. Due to its vast atmospheric monitoring network, the Auger Observatory is an interesting reference site for further atmospheric studies.

1. Introduction

Aerosols (particles suspended in the atmosphere) represent a significant constituent of the atmosphere that attenuates electromagnetic radiation in the Visible and UV ranges. Since the astronomical/astrophysical sites that include optical detectors of this radiation must be placed in very clean atmospheric regions of the globe, a detailed study of the aerosols of these regions is of major importance [1]. Besides, these sites offer an interesting test bed for aerosol research since they typically have many instruments in place for comparison. This work presents results of concentration and elemental characterization of aerosols collected at the Pierre Auger Observatory of cosmic rays, using experimental sampling techniques for the first time in a cosmic ray observatory. Gravimetric analysis was performed for obtaining aerosol concentration while elemental composition studies mainly focused on PIXE results and complemented with SEM/EDX results.

The Auger Project measures ultrahigh energy cosmic rays above 3×10^{18} eV, with special interest in the region of the GZK suppression (above 3×10^{19} eV) [2,3], in which previous experiments show severe discrepancies [4–6]. Scientists from 17 countries compose the Pierre Auger Collaboration (www.auger.org). The Auger Observatory, inaugurated in November 2008, is placed in the southern hemisphere, in the Pampa Amarilla plateau, near the city

* Corresponding author at: Instituto de Física Rosario, Bv. 27 de Febrero 210 bis. (2000) Rosario, Argentina. Tel.: +54 341 4472824x30/33.
E-mail address: micheletti@ifir-conicet.gov.ar (M.I. Micheletti).

0168-583X/$ - see front matter © 2012 Elsevier B.V. All rights reserved.
http://dx.doi.org/10.1016/j.nimb.2012.07.022

of Malargüe, Mendoza Province, Argentina. The Auger Observatory is at present being upgraded to extend its detection range to lower energies: 10^{17}–3×10^{18} eV [7,8]. It has a hybrid detection system composed of surface detectors (SD) and fluorescence detectors (FD). The SD are water Cherenkov cylindrical tanks distributed over an area of 3000 km^2 (that makes Auger the largest observatory in the world taking data at present), in a 1.5 km spaced triangular grid. The fluorescence system consists of 27 telescopes grouped in four stations ('eyes') which are placed on the perimeter of the SD array, looking over its area to detect nitrogen fluorescence light (in the range 300–450 nm) produced by the interaction of the cosmic ray showers with atmospheric nitrogen molecules [9].

It is extremely important to have reliable FD shower reconstructions. To reach such confidence in FD data, it is necessary to evaluate the most significant sources of error in FD reconstructions. An important one may arise when there is poor characterization of atmospheric transmission of fluorescence light. Since aerosols are highly variable with location and time (even during a day), a proper knowledge of them turns out to be critical for a good evaluation of atmospheric transmittance. Different techniques and devices have been designed for the Auger Observatory for the evaluation of the aerosol content and its distribution in height. These include a Raman LIDAR (Light Detection And Ranging) that operates only during non data-taking of cosmic ray showers periods, due to the interference caused by its high repetition-rate system, four elastic backscatter LIDAR instruments, each placed close to a corresponding FD eye, and the CLF (Central Laser Facility located near the center of the Auger array) and XLF (Extreme Laser Facility) that fire well calibrated laser beams into the sky [10,11]. These monitoring systems obtain the aerosol optical depth as a function of height. In turn, the HAM (Horizontal Attenuation Monitors) measure the horizontal attenuation length between the FD almost at ground level and the APF (Aerosol Phase Function Monitors) give the aerosol phase functions (that describe the angular distribution of aerosol diffused light). Other systems complete this complex setup, such as star monitors (that obtain the total optical depth from observation level to the top of the atmosphere) and cloud cameras [12,13].

The techniques mentioned above supply information about the bulk properties of aerosols as attenuators of the fluorescence radiation but do not characterize the aerosols themselves. Such characterization could help in the understanding of aerosol behavior in the attenuation process. In fact, some assumptions are made concerning the characteristics of the aerosols at the Auger Observatory, such as that they are desert type particles and that the same type of aerosols can be considered at all the FD eyes. Also, there are two second order corrections for which the shower reconstruction calculations assume the aerosols are purely scattering: multiple scattering and scattered Cherenkov light. It is possible that aerosol sampling measurements could improve these corrections.

In this work we intend to gain an insight into the real particles present at the Observatory, by capturing and analyzing them. The results add new information about the aerosols at the site and can be compared with information obtained by the instruments mentioned before, which do not discriminate the effect of the aerosol characteristics in the attenuation of fluorescence light in the atmosphere [14]. This information can give a clearer idea about the origin of the aerosols present at the Observatory, their sources and trajectories, and the connection between their type and the meteorological variables in the region. A knowledge of the aerosol type (elemental composition, shape, and size) turns out to be useful for a better knowledge of their effect in fluorescence light attenuation and, thus, in cosmic ray shower reconstruction. It can be critical in situations which differ significantly from the ones assumed as normal in calculations, like the presence of clouds of biomass burning aerosols (highly absorptive) in the region or volcanic ashes (the ones coming from the eruption of Chaitén volcano in May 2008 and Puyehue volcano in June 2011 passed near the region of the Observatory).

At the same time, a better knowledge of the aerosols at the Observatory site, supplied by the local detailed measurements presented in this work, can help in the understanding of the signals given by other aerosol monitors operating there, for example, it could provide information for obtaining the lidar ratio used in lidar analysis [15]. It could also help in the understanding of the phase function measurements given by the APF monitors. In addition, aerosol sampling at ground level, combined with a Raman LIDAR system planned for the Central Laser Facility could also improve identification of periods of extremely low aerosol concentration.

In Latin America there are few studies of atmospheric aerosol pollution and during recent years attention has been paid to air pollution in urban rather than non-urban communities, almost all made in mega-cities [16–19, and references therein, 20]. Very little effort has been made in the measurement of atmospheric aerosols in intermediate cities or rural areas. The only reported study of elemental composition of atmospheric aerosols was in the city Chillan, located on the Chilean side of the Andes [21].

2. Materials and methods

2.1. Collection of samples at the Auger Observatory

The samples correspond to the Southern Hemisphere winter and spring seasons –from June to November 2008– and were collected at the FD station of Coihueco (35° 06′ 52.9″ S, 69° 36′ 02.7″ W, 1712 m a.s.l.), on the roof of the FD building, 6.3 m above ground level. An Andersen-Graseby 240 dichotomous sampler (see Fig. 1) provided with polycarbonate membrane filters (Millipore® HTTP, diameter 37 mm, pore 0.4 μm) was used to separate fine size particles PM2.5 (with aerodynamic diameters $d \leqslant 2.5$ μm) and coarse particles PM2.5–10 ($2.5 < d \leqslant 10$ μm). The sampling period was 24 h, beginning at 12:00 a.m. of the initial day and ending at 12:00 a.m. of the next day. In this way, the whole night is included

Fig. 1. Andersen–Graseby 240 dichotomous sampler at the sampling site: the roof of the FD building at Coihueco, Auger Observatory.

in each sampling period. It is important to note that we are especially interested in the atmospheric situation at night because FD measurements are performed during the night. Also, in order to increase aerosol information related to FD measurements, the criterion used for the distribution of the sampling days was to collect preferably during the FD operation periods, complemented by some measurements outside these periods to continue monitoring the aerosol evolution. The operational or actual flow rate is 16.7 l/min. The operational flow rate *Qa* was corrected to U.S. EPA reference conditions (298 K and 760 mm Hg) for the actual reported data, in order to obtain the standard flow rate *Qstd* used in the calculations of mass and elemental concentrations. The corresponding relationship is $Qa = Qstd\ (Ta/Pa).(760/298)$, where *Ta* and *Pa* are the actual temperature and pressure for each measurement. The pressure correction is important due to the altitude of the measurement site mentioned above.

2.2. Gravimetric analysis

For gravimetric analysis and mass concentration measurements, a total of 34 filters containing fine particles (PM2.5) and 38 filters containing coarse particles (PM2.5–10) were considered. Filters of fine and coarse particles and PM10 were obtained concurrently over 33 days. The deposited mass in each sample was determined as the difference between the mass of the filter with the aerosols in it and the mass of the filter before the aerosol collection, using a microbalance (Microbalance M3, with a precision of ±1 μg). Before weighing, filters were conditioned (humidity 50% and temperature 25 °C during at least 24 h) and irradiated with an alpha source (^{238}U) to eliminate static charge on them during weighing. Then, the PM2.5 and PM2.5–10 concentrations, expressed as μg m^{-3}, were calculated as the ratio between the mass collected and the volume of air that passed through the sampler instrument during each period of measurement. The PM10 concentration in the ambient air is then computed as the sum of PM2.5 and PM2.5–10 concentrations (the net mass collected on both, the filters with coarse and fine particles, divided by the volume of the air sampled). The total volume of air sampled is considered for the standard conditions (*Vstd*) and it is determined from the standard total flow rate and the sampling time.

2.3. PIXE measurements

The collected PM2.5 and PM2.5–10 samples were further studied for elemental composition (from *S* up) by means of the PIXE technique [22] and, subsequently, atmospheric elemental concentrations were computed. PIXE experiments took place at the TANDAR Laboratory accelerator facility of the Comisión Nacional de Energía Atómica, Buenos Aires, Argentina, as it was done in previous works (for example, [23–25]). PIXE analysis was performed (on 19 filters of each fraction) by using heavy ions ^{16}O (7+ charge state) at 50 MeV energy. Elements, namely (S, Cl, K, Ca, Ti, Mn and Fe) were studied in PM2.5 and PM2.5–10 samples collected on polycarbonate filters.

Targets were placed at 90° with respect to the incoming beam and the induced X-rays were measured using an EG&G Ortec Si(Li) detector (sensitive area of 80 mm^2, 12.5 μm Be window), with a resolution of 220 eV at 5.9 keV (Kα Mn line). The detector was placed at 135° with respect to the beam direction, outside the reaction chamber, at 5 cm from the target. The transmitted projectile ions were collected in a Faraday cup placed downstream from the target, to measure the integrated charge. A beam collimated to a 3 mm diameter, currents of about 4 nA and integrated charges from 1 to 2.5 μC were used.

SEM visual observations show that at microscopic level, irregular particulate distributions can occur in regions of tens or few hundreds of microns length (especially for thin samples). With the beam diameter used for PIXE, the deposits can be considered uniformly distributed. On the other hand, during the irradiation the filter was moved in front of the beam so that most of the area of the deposit was sampled. This motion also allowed us to work with higher currents, to avoid possible beam damage to the filters and to average the X-ray production on the sample.

The X-ray identification was performed using experimental energies obtained from thin film standards supplied by MicroMatter^R made from single elements (Ti, Cr, Fe, Pb) or compounds (PGa, CuS_X, KCl, CaF_2), evaporated onto thin Mylar^R backings with thickness in the order of 50 μg/cm^2, certified to 5%.

PIXE analysis was performed directly on the particle filter. The thicknesses of the measured particulate deposits were in all cases lower than 1 mg/cm^2. For this reason, the concentrations [μg/m^3] were determined using the thin sample criterion, by comparison with the certified standards.

We perform the measurements of the standards and samples with the same beam and the same X-ray detector, without changing the experiment geometry.

The PIXE analysis provides elemental concentrations in mass per unit area on the filters. The concentrations in mass per unit volume of sampled air are calculated from these using the corrected flow rate, sampling time, and the areas of the deposits on the filters. The energies and photo-peaks areas of the resulting PIXE spectra were analyzed with the WinQxas 1.40 computer code developed by IAEA (with modified cross sections for ^{16}O at 50 MeV [26]).A standard target of the element *i* with an elemental thickness $(\rho x)_{S,i}$ [μg/cm^2] gives after collection of a total charge$Q_{S,i}$:

$$Y_{S,i} = \frac{Q_{S,i}}{q \cdot e} \cdot \frac{N_A}{A_i} \cdot (\rho x)_{S,i} \cdot (\varepsilon \cdot \sigma)_{S,i}$$

where $Y_{S,i}$ is the detected number of X-rays (the area of the peak of the X-line *i* calculated with WinQxas), *q* is the charge state of the ^{16}O ion, *e* the elemental charge, N_A Avogadro's number, A_i the atomic mass of target element, ε is the absolute detection system efficiency for the X-line of the element *i* (window absorption is automatically included) and σ is the corresponding X-ray production cross section.

Therefore, comparing the X-ray production of each element in the standard and the sample (*S* refers to the standard and *X* to the sample):

$$(\rho x)_{X,i} = (\rho x)_{S,i} \cdot \frac{Y_{X,i}}{Y_{S,i}} \cdot \frac{Q_{S,i}}{Q_X}$$

which gives the unknown thickness from the measured peak areas and total collected charges.The measured elemental thickness $(\rho x)_{X,i}$ is multiplied by the area of the filter exposed to the air carrying the particulate matter inside the tubes of the Andersen-Graseby 240 dichotomus sampler (area of the deposit on the filter, A_{dep}). The result is then divided by the total volume of air sampled considered for the standard conditions, to obtain the elemental concentration (in mass per cubic meter) for each element $C_{X,i}$:

$$C_{X,i} = (\rho x)_{X,i} \cdot A_{dep} / Vstd_X$$

A_{dep} is the same for all the samples. It is fixed by the Andersen-Graseby 240 filter holders design and was measured with 0.2 mm error with a Vernier caliper.

The concentrations of elements were calculated within an experimental error ranging between 10% and 20%. The most important contributions to the errors of the final concentrations are coming from: air volume sampled (4%), fit of the X-ray peaks in the spectra (between 2% and 17% depending on the local background and the intensity of each line in the spectrum), mass determination by weighting (specially the thin samples) and calibration standards

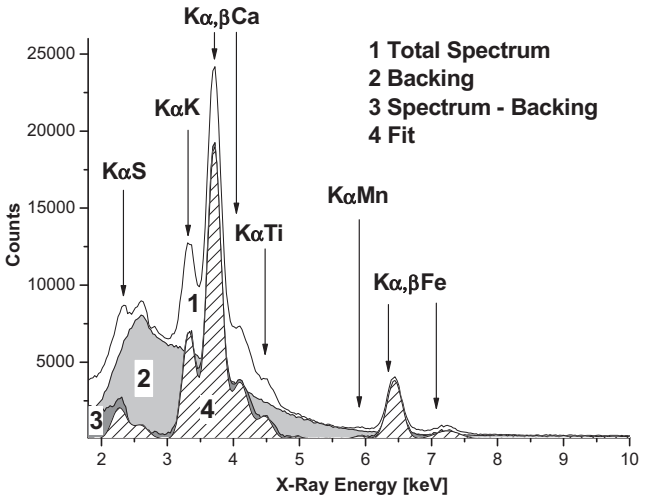

Fig. 2. Typical aerosol PIXE spectra obtained using 50 MeV ^{16}O ions. (1) Spectrum from a typical aerosol measured in the present work, (2) Backing (Millipore^{R} substrate) spectrum (light gray), (3) Clean spectrum, resulting from the subtraction of the spectra (1) and (2) (dark gray) and (4) fit of spectrum (3) (lined).

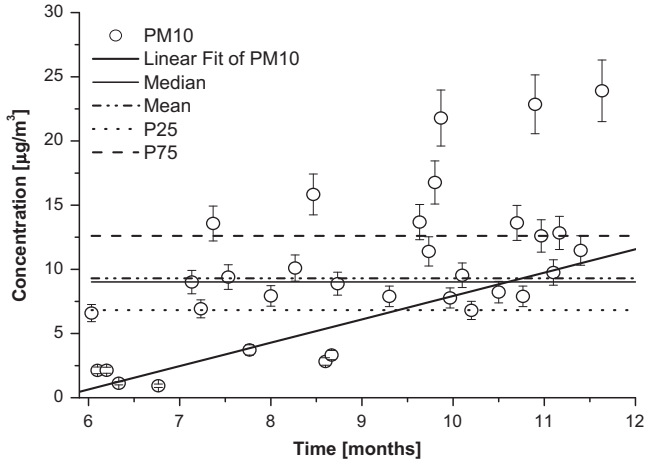

Fig. 3. Aerosol mass concentration for PM10 particulate measurements at the Coihueco sampling site. P25 and P75 are the 75% percentile and the 25% percentile values respectively. The linear fit of PM10 values shows a trend towards increased concentration from winter to spring.

(5%). Corrections for dead time were included in the determination of the line intensities. We consider only elements whose normalized intensities were higher than 3σ (σ corresponds to one standard deviation of the background window under the peak). Detection limits vary between 1 μg m^{-3} (Ti) and 3 μg m^{-3} (S). More details of the experimental setup can be found elsewhere [18].

Fig. 2 shows the PIXE spectra from a typical aerosol sample and its backing (blank filter Millipore) obtained using 50 MeV ^{16}O ions. The spectra are normalized to charge and live-time. In addition, it is shown the clean spectrum with the subtracted backing and the corresponding fit.

2.4. SEM measurements

Particle morphology and elemental composition were also studied as a complement to PIXE analysis using a Scanning Electron Microscope (Philips SEM 515) equipped with an Energy Dispersive X-ray system (EDAX Falcon PV 8200), provided with a Si(Li)-Be window detector. With this arrangement, the detection of elements of Atomic Number (Z) higher than 11 (Na) is possible. Semi-quantitative standarless analysis with ZAF factors (Atomic Number – Absortion – Fluorescence) for matrix correction was used for composition calculations. SEM – EDX techniques were performed in a few filters previously coated with Ag for conductivity.

2.5. Data analysis

Data from both PM2.5 and PM2.5–10 fractions were characterized by mean, median, percentiles, maximum, minimum, outlier and extreme values. These parameters were illustrated by Box–Whisker plots. Statistical analysis was performed by using Statistica 7.1 software (StatSoft, Inc.).

3. Results and discussion

3.1. Mass concentrations

The measured aerosol mass concentrations PM10 (=PM2.5 + PM2.5–10 fractions) collected in the period 1 June to 19 November 2008 are shown in Fig. 3. This figure shows mean, median, 25 and 75 percentiles and a linear fit of the PM10 values for the winter and spring months. Low aerosol concentrations are observed, ranging from 0.9 to 24 μg/m^3. The mean value for the period of this study is [mean(se)] 9.8(1.0) μg/m^3 [sd = 5.9 μg/m^3]. The mean value during winter is 7(1.1) μg/m^3 [sd = 4.5 μg/m^3], about half of the 13.1(1.5) [sd = 5.7 μg/m^3] measured during springtime at the same monitoring site. The mean value of the PM2.5 fraction is 2.8(0.4) μg/m^3 [sd = 2.5 μg/m^3] and the mean value of the PM2.5–10 fraction is 7.2(0.9) μg/m^3 [sd = 5.5 μg/m^3]. Examining the percentage contributions of the two components, the PM2.5 fraction represents approximately the 30% of the PM10 fraction.

The linear fit of Fig. 3 shows a trend towards increased concentration from winter to spring, which may be related to decreased snowfall and increased temperature. Although snowfalls are scarce during winter, the low temperatures keep the snow for long periods, reducing atmospheric particulates near the surface.

The climate of the region is continental arid and very dry. The average temperature is 20 °C in January while in July it is 3 °C. The average annual precipitation (rain and snow) is approximately 240 mm and its distribution is heterogeneous. Precipitation is greatest between May and October (snow). During the summer, rain periods are short and intense. The average annual temperature is 12.5 °C.

The concentrations of PM reported in this study are significantly lower than those measured at Chillán, another Andean site [21]. Low values of PM2.5, comparable to those found at the Auger Observatory during the winter – spring period of 2008, have been observed in summer at some bases in the Antarctic Peninsula ([27] and references therein) where PM2.5 levels of ~2 μg m^{-3} were found near the Chilean Bernardo O'Higgins base in the interior of the Antarctic Peninsula during the summers of the years 2006 and 2007.

3.2. Elemental composition

As stated in paragraph 2.3, PIXE was applied to study the elemental concentrations of the collected samples of aerosols.

A statistical summary of elemental concentrations (ng/m^3) as a result of the PIXE analysis on aerosol samples is shown in Table 1. The results correspond to 19 aerosol samples of each fraction collected at the Auger cosmic ray observatory between 1 June and 22 August 2008.

The sum of the element concentrations measured by PIXE represents 25% and 13% of the PM2.5 and PM2.5–10 total mass respec-

Table 1
Elemental concentrations (ng/m^3), as given by the analysis with the PIXE technique.

	PM2.5 [ng/m^3]			PM2.5–10 [ng/m^3]		
	Mean (SD)	Min	Max	Mean (SD)	Min	Max
Mass	1540 (1150)			6136 (6182)		
S	210 (143)	81	626	228 (283)	12	1113
Cl	67 (50)	11	131	148 (142)	10	439
K	46 (40)	0.7	143	114 (109)	4	318
Ca	41 (53)	3	183	236 (215)	8	657
Ti	4 (6)	0.1	15	18 (16)	0.3	42
Mn	2 (2)	0.2	5	4 (4)	0.5	12
Fe	11 (13)	0.7	39	62 (53)	3	192
	25%			13%		
	Median (SD)	P25	P75	Median (SD)	P25	P75
S	164	131	249	113	71	302
Cl	48	27	129	99	63	209
K	40	17	66	72	28	199
Ca	27	14	30	155	77	428
Ti	2	0.2	7	14	1.3	36
Mn	0.8	0.7	0.9	3	1.3	6
Fe	9	1	2	52	24	86

tively. The rest of the mass are low Z elements which cannot be detected by our X-ray setup. Fig. 4 shows the levels of some elements (S, Cl, K, Ca, Ti, Mn, Fe) in PM2.5 and PM2.5–10 fractions.

Among the elements detected by PIXE, S is the one with the highest concentration in the fine fraction while Ca is the one with the highest concentration in the coarse one.

The following are some considerations about the box plot (Fig. 4).

A data point value (DPV) is deemed to be an outlier if the following conditions hold:

$$\mathrm{DPV} > \mathrm{UBV} + 1.5 \cdot (\mathrm{UBV} - \mathrm{LBV}) \text{ or}$$
$$\mathrm{DPV} < \mathrm{LBV} - 1.5 \cdot (\mathrm{UBV} - \mathrm{LBV})$$

On the other hand, a DPV is deemed to be an extreme value if the following conditions hold:

$$\mathrm{DPV} > \mathrm{UBV} + 2 \cdot 1.5 \cdot (\mathrm{UBV} - \mathrm{LBV}) \text{ or}$$
$$\mathrm{DPV} < \mathrm{LBV} - 2 \cdot 1.5 \cdot (\mathrm{UBV} - \mathrm{LBV})$$

UBV and LBV are the upper (the 75% percentile) and the lower (the 25% percentile) values of the box, respectively. The 1.5 value is called outlier coefficient.

The non-outlier range is the range of values that fall below the upper outlier limit and above the lower outlier limit. That is, the upper limit of the whisker is the first data point value that fall below the upper outlier limit, while the lower limit of the whisker is the first data point value above the lower outlier limit.

Table 2 shows the average composition determined by SEM/EDX in two samples, one of each PM fraction. On selected areas of the PM2.5 and PM2.5–10 samples, 35 and 50 particles were analyzed, respectively. Si, Al, Ca, Mg and Fe, the typical mineral soil elements, are the major components, so we can suppose that collected particles are mainly suspended dust. Some particles in both fractions which give no detectable X-ray signal may be composed of light elements (Z < 11), presumably organic matter.

PM2.5 fraction shows more undetected particles. This may be due to the fact that insufficient precision is attainable with this EDX arrangement when focusing the beam on particles smaller than 1–2 μm. Thus, it is not feasible to get a proper X-ray signal of any element in many of them. Consequently, as all analyzed particles are included in the calculation, the sum of elemental percentages is often lower than 100, being difficult to reach to a conclusion about the presence of organic matter in this fraction.

Comparison of these results with PIXE shows that in PM2.5–10 samples, the major elements Si and Al may account for the

Table 2
Average particle concentrations (atomic percentages) of PM2.5 and PM2.5–10 fractions, obtained by EDX applied to two samples, one of each PM fraction.

Fraction	Mg	Al	Si	P	S	K	Ca	Fe	Sum
PM2.5	3.5	11.1	60		1.2		6.3		82
PM2.5–10	4.4	16.3	69.4	0.74	0.34	0.54	4.6	3.7	100

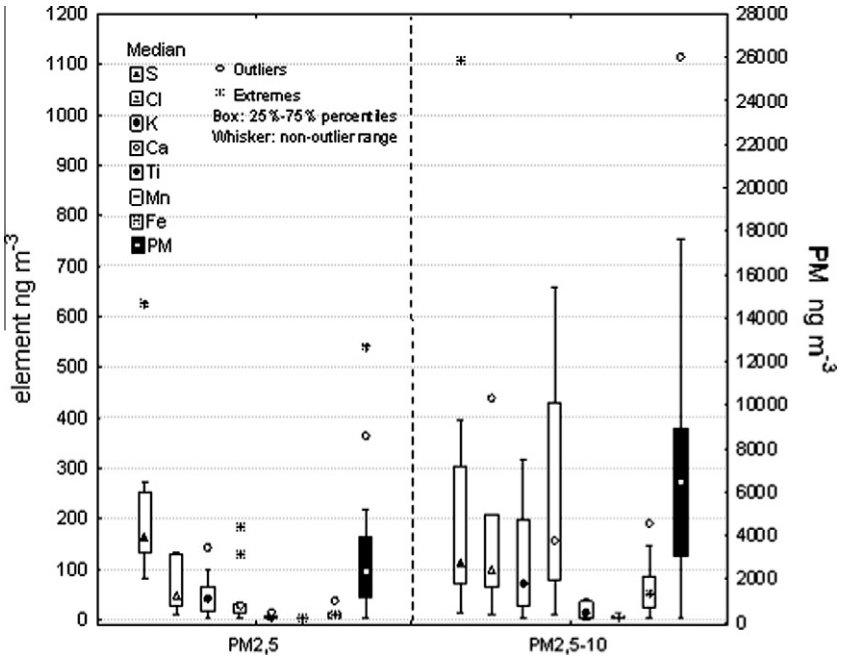

Fig. 4. PM and elemental concentrations observed at the Pierre Auger Observatory (Coihueco site) during a monitoring field campaign carried out from 1 June to 22 August 2008.

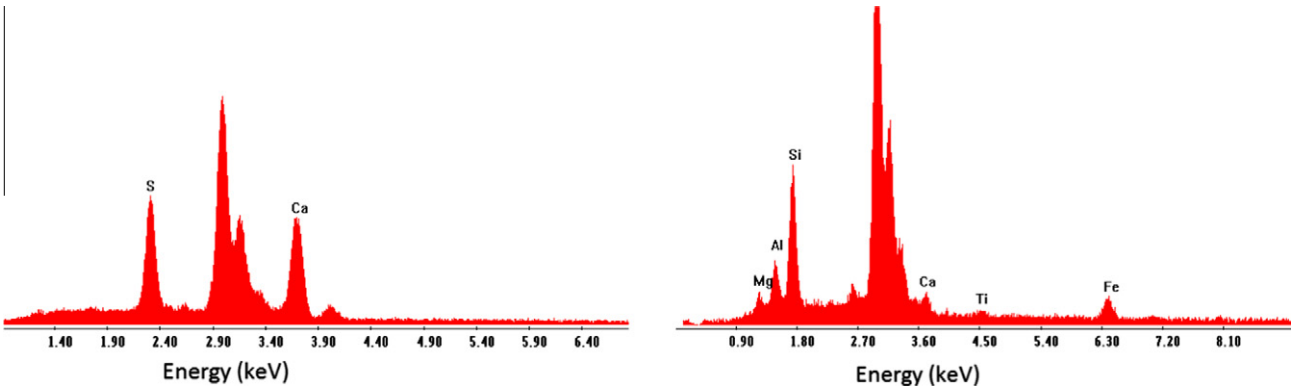

Fig. 5. Left: SEM/EDX spectrum of a particle of the sample of PM2.5–10 collected on 1 June 2008. It contains S and Ca in relation 1:1. Right: SEM/EDX spectrum of an aluminosilicate of the sample of PM2.5–10 of 8 August 2008. The vertical axis corresponds to the intensity (counts per second). The higher peak in both spectra is due to the silver sputtering performed on the samples.

remaining mass. For fine fractions this is not so clear due to the poor focusing conditions mentioned above.

Some individual particles in other samples corresponding to the same period were also analyzed; general results obtained are in accordance with data presented in Table 2. As was previously told most single particles were mainly composed by Si and Al (aluminosilicates) with minor percentages of Ca, Mg and Fe. There are some Fe rich grains. There are also some Calcium rich particles, sometimes associated with high Sulfur content, which may indicate the presence of a Ca–S compound. It is worth mentioning that the soil of the region under study contains Calcium sulfate ($CaSO_4$) and that there are gypsum factories in the area. Fig. 5 left is an example of a SEM/EDX spectrum of a particle that contains Ca and S in atomic relation 1:1 (atomic percentages in proportion of about 50–50%) and which is supposed to be of Calcium sulfate (the small peak after the highest Ca peak, also belongs to Ca). Fig. 5 right is an example of a SEM/EDX spectrum of an aluminosilicate.

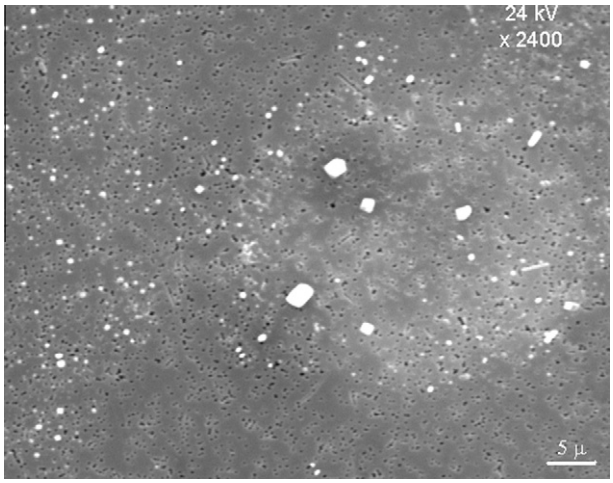

Fig. 6. SEM micrographs of particles of NaCl found on the sample of PM2.5 of 20 August 2008, in which the characteristic cubic shape of NaCl crystals is observed.

NaCl crystals were also detected. Most probably, their origin could be in the salt flats of the region. But they could also arrive from the Pacific Ocean, being transported by air masses at great altitude. A backward trajectory analysis (not shown) [28] of air masses effectively supports the latter conclusion. Part of the S found could also have a marine origin in the form of sulfate salts. Most of the back trajectory analyses performed for the period under study, showed winds arriving at the sampling site from the west, either from the ocean or from the north-west Andean region. The latter is the most frequent origin found for the winds arriving at the Observatory on the sampling days during the winter – spring period analyzed in this work, suggesting that they carry the Andean minerals. It may be mentioned that the soil of the region under study has a volcanic origin. Fig. 6 shows a SEM micrograph in which the characteristic cubic shape of NaCl crystals is observed. The SEM/EDX analysis performed on them, with the correction of the ZAF factors (as mentioned in Section 2.4), shows the presence of Na and Cl in relation 1:1.

Uncertainties associated with X-ray microanalysis are widely dependent on the elements and their relative concentrations. Errors range from 1% to 10% relative for major elements to much higher values for minor concentrations.

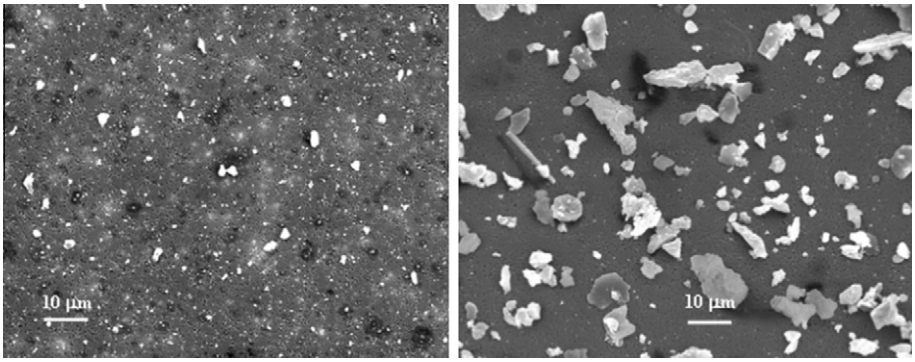

Fig. 7. Left: SEM micrograph of PM2.5 fraction, collected on 7 July 2008. Right: SEM micrograph of PM2.5–10 fraction, collected on 27 October 2008.

SEM micrographs of two representative PM2.5 and PM2.5–10 samples are shown in Fig. 7.

4. Conclusions

This experimental work adds new information which is complementary to that obtained by the aerosol monitors at the Auger Observatory. For the first time, the aerosols of the site were collected on filters and then analyzed by different techniques: gravimetry, PIXE and SEM/EDX. These first local detailed aerosol measurements, expand the description of the atmosphere at the site of the Observatory, which has an extensive data base of measurements of bulk aerosol properties. Concentration of aerosols and their elemental composition were obtained. It is worth pointing out that this is the first study of this type performed at a cosmic ray observatory.

This work describes the method used for the analysis of samples of collected aerosols and sets this work up for an interesting future paper comparing the bulk and local measurements.

Low concentrations of aerosols were measured during winter and spring 2008 (period from 1 June to 19 November, 2008) at the Auger Observatory. The mean value of PM10 found for the period of this study was [mean(se)] 9.8(1.0) $\mu g/m^3$ [sd = 5.9 $\mu g/m^3$]. The mean value during winter was 7(1.1) $\mu g/m^3$ [sd = 4.5 $\mu g/m^3$], about half of the 13.1(1.5) $\mu g/m^3$ [sd = 5.7 $\mu g/m^3$] measured during springtime. The PM2.5 fraction was approximately 30% of the PM10 fraction. Even when the aerosols can vary significantly over a few days or even hours, due to winds, rainfall, the arrival of contamination clouds to the site, etc., we can nevertheless observe a general trend of increasing concentrations from winter to spring. The increase of the aerosol content in warmer seasons is in accordance with the measurements of other aerosol monitors of the Auger South Observatory, like those that obtain aerosol optical depths [14].

PIXE results give the levels of S, Cl, K, Ca, Ti, Mn, Fe that are present in the analyzed aerosol samples, corresponding to the period from 1 June to 22 August 2008, showing that these elements correspond to 25% and 13% of the PM2.5 and PM2.5–10 total mass, respectively. The rest of the mass is due to elements with low Z (below 16) which cannot be detected by our X-ray setup. Comparison with SEM/EDX analysis shows that most of them are Si and Al (aluminosilicates).

Among the elements detected by PIXE, S is the one with the highest concentration in the fine fraction while Ca is the one with the highest concentration in the coarse one.

Analysis of individual particles with SEM/EDX complements PIXE results. The SEM/EDX analysis is important for major elements analysis improving the understanding of the mass not detected by PIXE. From EDX it can be concluded that most of the collected particles are suspended mineral dust from the soil of this Andean desert region. Some particles in both fractions which give no detectable X-ray signal may be composed of light elements ($Z < 11$), presumably organic matter. Particles whose EDX spectra are in accordance with the Calcium sulfate spectrum were found frequently. Their origin can be from the soil of the region as it contains this compound and they are probably generated during its extraction at the gypsum factories. A few Sodium Chloride crystals were also observed. They most probably come from the salt flats found in the surrounding area but may also come from the Pacific Ocean, carried by winds, which in the region of study arrive mostly from the west on the analyzed days of the winter–spring period.

Our results indicate that most of the aerosols at the Auger Observatory come from the soil of the region, supporting the conclusion that the extremely low aerosol concentration values found during the colder winter periods is due to the snow that keeps them captured in the surface.

In Latin America there are few studies of this type and almost all of them were performed in highly populated cities. Thus, this study represents a contribution to the knowledge of the situation of non-urban regions of mountain and desert types at mid-latitudes of the continent.

Future work will take into account the morphological analysis of aerosols, complementing the elemental analysis presented in this work, and giving new insight on their role on attenuation of UV fluorescence light produced by cosmic rays. This experiment was performed at the Auger Observatory, in order to supply information that can be used to try to gain insight on the effect that aerosols play in the attenuation of this light. This Observatory is an excellent site for general atmospheric analysis thanks to its vast network of atmospheric monitoring devices, whose results can be used also for climate change studies [29] and solar UV radiation attenuation [30]. At present, the interest of the Auger Observatory for interdisciplinary science is being discussed [31] and the collaboration with atmospheric scientists is planned to be strenghtened. The analysis of collected aerosols presented here is the initial one of this type and it is planned that ill will be continued and integrated with a larger aerosol sampling program that is being designed.

Acknowledgments

We want to acknowledge the support from the following institutions in Argentina: CNEA, CONICET, ANPCYT, Laboratorio Tandar/CNEA, Universidad Nacional de Rosario, Universidad Nacional de Gral. San Martín.

We acknowledge the technical help of Pedro Barraza, of Pierre Auger Observatory and the discussions with the geologist Jorge A. Caviedes Vidal, of the Technical School N° 4-018 "M. N. Savio", Malargüe, about the soil of the region under study.

References

[1] F. Esposito, S. Mari, G. Pavese, C. Serio, Diurnal and nocturnal measurements of aerosol optical depth at a desert site in Namibia, Aerosol Sci. Technol. 37 (2003) 392–400.
[2] K. Greisen, End to the cosmic-ray spectrum?, Phys Rev. Lett. 16 (1966) 748–750, http://dx.doi.org/10.1103/PhysRevLett.16.748.
[3] G.T. Zatsepin, V.A. Kuz'min, Upper limit of the spectrum of cosmic rays, JETP Lett. 4 (1966) 78–80.
[4] M. Takeda et al., Extension of the cosmic-ray energy spectrum beyond the predicted Greisen–Zatsepin–Kuz'min Cutoff, Phys. Rev. Lett. 81 (1998) 1163–1166, http://dx.doi.org/10.1103/PhysRevLett.81.1163.
[5] N. Sakaki et al. (AGASA Collaboration), Energy estimation of AGASA events, Proc. 27th ICRC, Hamburg, Germany (2001) 329–332.
[6] D.R. Bergman, (HIRes Collaboration), Monocular UHECR spectra as measured by HIRes, Nucl. Phys. B – Proc. Suppl. 117 (1) (2003) 106–108, http://dx.doi.org/10.1016/S0920-5632(03)90500-7.
[7] H. Klages, for the Auger Collaboration, HEAT: enhancement telescopes for the P. Auger southern Observatory enhancements, in: Proc. 30th ICRC, Mérida, México, 2007.
[8] A. Etchegoyen, for the Auger Collaboration, AMIGA: a muon detector and infilled array for the Auger Observatory, in: Proc. 30th ICRC, Mérida, México, 2007.
[9] The Auger Collaboration, The Pierre Auger Observatory Design, Report, March 14, 1997.
[10] B. Fick, M. Malek, L.A.J. Matthews, J. Matthews, R. Meyhandan, M. Mostafa, M. Roberts, P. Sommers, L. Wiencke, The central laser facility at the Pierre Auger Observatory, J. Instrum. 1 (2006) 11003, http://dx.doi.org/10.1088/1748-0221/1/11/P11003.
[11] L. Wiencke, For the Auger Collaboration, Extracting first science measurements from the southern detector of the Pierre Auger Observatory, Nucl. Instrum. Meth. A 572 (1) (2007) 508–510, http://dx.doi.org/10.1016/j.nima.2006.10.318.
[12] S.Y. BenZvi et al., Measurement of aerosols at the Pierre Auger Observatory, in: Proc. 30th ICRC, Mérida, México, 2007.
[13] S.Y. BenZvi, for the Auger Collaboration, Atmospheric monitoring and its use in air shower analysis at the Pierre Auger Observatory, in: 31st ICRC, Lódz, Poland, 2009.
[14] The Auger Collaboration, A study of the effect of molecular and aerosol conditions in the atmosphere on air fluorescence measurements at the Pierre

Auger Collaboration, Astropart. Phys. 33 (2010) 108–129, http://dx.doi.org/10.1016/j.astropartphys.2009.12.005.
[15] R. Mussa, the Auger Collaboration, Atmospheric monitoring for the Pierre Auger Observatory, Nucl. Phys. B (Proc. Suppl.) 190 (2009) 272–277, http://dx.doi.org/10.1016/j.nuclphysbps.2009.03.099.
[16] S. Reich, F. Robledo, D. Gómez, P. Smichowski, Air pollution sources of PM10 in Buenos Aires City, Environ. Monit. Assess. 155 (2008) 191–204, http://dx.doi.org/10.1007/s10661-008-0428-x.
[17] J.F. Magallanes, L. Murruni, D. Gómez, P. Smichowski, R. Gettar, An approach to air pollution source–receptor solution by angular distances, Water, Air, Soil Pollut. 188 (2008) 235–245, http://dx.doi.org/10.1007/s11270-007-9540-8.
[18] L.G. Murruni, V. Solanes, M. Debray, A.J. Kreiner, J. Davidson, M. Davidson, M. Vázquez, M. Ozafrán, Concentrations and elemental composition of particulate matter in the Buenos Aires underground system, Atmos. Environ. 43 (2009) 4577–4583, http://dx.doi.org/10.1016/j.atmosenv.2009.06.025.
[19] M. Dos Santos, D. Gómez, L. Dawidowski, E. Gautier, P. Smichowski, Determination of water-soluble and insoluble compounds in size classified airborne particulate matter, Microchem. J. 91 (2009) 133–139, http://dx.doi.org/10.1016/j.microc.2008.09.001.
[20] D. Morata, M. Polvé, A. Valdés, M. Belmar, M.I. Dinator, M. Silva, M.A. Leiva, T. Aigouy, J.R. Morales, Characterisation of aerosol from Santiago, Chile: an integrated PIXE–SEM–EDX study, Environ. Geol. 56 (2008) 81–95, http://dx.doi.org/10.1007/s00254-007-1141-8.
[21] O.F. Carvacho, K. Trzepla-Nabaglo, L.L. Ashbaugh, R.G. Flocchini, P. Melín, J. Celis, Elemental composition of springtime aerosol in Chillán, Chile, Atmos. Environ. 38 (2004) 5349–5352, http://dx.doi.org/10.1016/j.atmosenv.2004.03.076.
[22] S.A.E. Johansson, J.L. Campbell, PIXE: A Novel Technique for Elemental Analysis, John Wiley and Sons, Inc., New York, 1988.
[23] A. Caridi, A.J. Kreiner, J. Davidson, M. Davidson, M. Debray, D. Hojman, D. Santos, Determination of atmospheric lead pollution of automotive origin, Atmos. Environ. 23 (1989) 2855–2856, http://dx.doi.org/10.1016/0004-6981(89)90566-0.
[24] M.J. Ozafrán, M.E. Vázquez, A.J. Kreiner, M.E. Debray, J.M. Kesque, A.S.M.A. Romo, C. Pomar, H. Somacal, M. Davidson, J. Davidson, PIXE analysis of heavy water from a nuclear power plant, Nucl. Instrum. Meth. B 74 (4) (1993) 542–544, http://dx.doi.org/10.1016/0168-583X(93)95953-3.
[25] M.J. Ozafrán, M.E. Debray, R. Eusebi, A.J. Kreiner, M.E. Vázquez, A. Burlón, P. Stoliar, K X-ray production induced by ^{12}C on several elements, Nucl. Instrum. Meth. B 201 (2) (2003) 317–324, http://dx.doi.org/10.1016/S0168-583X(02)01738-X.
[26] M.J. Ozafrán, M.E. Vázquez, A.S.M.A. Romo, M.A. Cardona, M.E. Debray, D. Hojman, J.M. Kesque, A.J. Kreiner, J.J. Menendez, H. Somacal, J. Davidson, M. Davidson, Heavy ion induced X-ray emission work at the TANDAR laboratory in Buenos Aires, Nucl. Instrum. Meth. B 99 (1995) 384–386, http://dx.doi.org/10.1016/0168-583X(95)00324-X.
[27] M. Préndez, J. Wachter, C. Vega, R.G. Flocchini, P. Wakayabashi, J.R. Morales, PM2.5 aerosols collected in the Antarctic Peninsula with a solar powered sampler during austral summer periods, Atmos. Environ. 43 (2009) 5575–5578, http://dx.doi.org/10.1016/j.atmosenv.2009.07.030.
[28] HYSPLIT Model, Version 4 (National Oceanic and Atmospheric Administration, Air Resources Laboratory NOAA-ARL, http://www.arl.noaa.gov/ready/hysplit4.html).
[29] R. Turco, Aerosols and clouds, in: G. Brasseur, J. Orlando, G. Tyndall (Eds.), Atmospheric Chemistry and Global Change, Oxford University Press, New York, 1999, pp. 117–157.
[30] M.I. Micheletti, E. Wolfram, R.D. Piacentini, A. Pazmiño, E. Quel, V. Orce, A. Paladini, The incidence of erythemal and UV solar irradiance over Buenos Aires, Argentina, J. Opt. A: Pure Appl. Opt. 5 (2003) S262–S268, http://dx.doi.org/10.1088/1464-4258/5/5/376.
[31] K. Louedec, for the Auger Collaboration, Atmospheric monitoring at the Pierre Auger Observatory – status and update, 32nd ICRC, Beijing, China, 2011.